

# Haploinsufficiency of *Runx1/AML1* promotes myeloid features and leukaemogenesis in BXH2 mice

Namiko Yamashita,<sup>1,2</sup> Motomi Osato,<sup>1,3</sup>  
Liqun Huang,<sup>3</sup> Masatoshi Yanagida,<sup>1,2</sup>  
Scott C. Kogan,<sup>4</sup> Masayuki Iwasaki,<sup>5</sup>  
Takuro Nakamura,<sup>5</sup> Katsuya Shigesada,<sup>2</sup>  
Norio Asou<sup>6</sup> and Yoshiaki Ito<sup>1,3</sup>

<sup>1</sup>Institute of Molecular and Cell Biology, Singapore, <sup>2</sup>Institute for Virus Research, Kyoto University, Kyoto, Japan, <sup>3</sup>Oncology Research Institute, National University of Singapore, Singapore, <sup>4</sup>Comprehensive Cancer Center, University of California, San Francisco, CA, USA, <sup>5</sup>The Cancer Institute, Japanese Foundation for Cancer Research, Tokyo, and <sup>6</sup>Department of Internal Medicine II, Kumamoto University School of Medicine, Kumamoto, Japan

Received 30 June 2005; accepted for publication 31 August 2005

Correspondence: Yoshiaki Ito, Institute of Molecular and Cell Biology, 61 Biopolis Drive, Singapore 138673, Singapore. E-mail: itoy@imcb.a-star.edu.sg

## Summary

Haploinsufficiency of *RUNX1/AML1* is associated with familial platelet disorder with a predisposition to acute myeloid leukaemia (FPD/AML), but the causal relationship remains to be addressed experimentally. Mice heterozygous for the *Runx1* null mutation, *Runx1*+/-, are considered to be genetically comparable with human FPD/AML patients but do not develop spontaneous leukaemia. To induce additional genetic alterations, retroviral insertional mutagenesis was employed with the use of BXH2 mice, which develop myeloid leukaemia because of the random integration of retrovirus present in the mouse. Heterozygous disruption of *Runx1* in BXH2 mice resulted in a shortening of the latency period of leukaemia. In addition, BXH2-*Runx1*+/- mice exhibited more marked myeloid features than control mice. Moreover, the *c-Kit* gene, mutated in human RUNX leukaemias, was recurrently activated in BXH2-*Runx1*+/- mice, and a colony-forming assay revealed synergism between the *Runx1*+/- status and c-KIT overexpression. In conclusion, the BXH2-*Runx1*+/- system is a promising mouse model to investigate the mechanism of leukaemogenesis in FPD/AML.

**Keywords:** AML1, Runx, CBF, familial platelet disorder, mutagenesis.

*RUNX1/AML1*, a key factor in the generation and maintenance of haematopoietic stem cells, is frequently mutated in human leukaemias (Okuda *et al*, 1996; Look, 1997; Speck & Gilliland, 2002; Ichikawa *et al*, 2004). *RUNX1* encodes the  $\alpha$ -subunit of the Runt domain transcription factor, PEBP2/CBF, and is the most frequent target of chromosomal translocations associated with leukaemias. The t(8;21), t(3;21) and t(12;21) rearrangements generate *RUNX1-ETO*, *RUNX1-EV11* and *TEL-RUNX1* chimaeric genes respectively (Look, 1997; Speck & Gilliland, 2002). The  $\beta$ -subunit, *PEBP2/CBFB*, which does not bind DNA, is also involved in leukaemias associated with inv(16), which generates the *PEBP2/CBFB-MYH11* chimaeric gene (Liu *et al*, 1993). Ample evidence shows that in most cases these chimaeric genes dominantly repress *RUNX1* function. For example, mice heterozygous for *RUNX1-ETO* or *PEBP2/CBFB-MYH11* knock-in constructs exhibit embryonic lethality with a phenotype similar to that of *Runx1* null mutants (Castilla *et al*, 1996; Okuda *et al*, 1996; Yergeau *et al*, 1997). In addition, *RUNX1* point mutations have been associated with the development of sporadic acute myeloid leukaemia (AML)

(Osato *et al*, 1999; Preudhomme *et al*, 2000). Germline mutations of *RUNX1* are correlated with familial platelet disorder with propensity towards AML (FPD/AML) (Song *et al*, 1999). As these mutations usually confer a monoallelic loss-of-function phenotype (Michaud *et al*, 2002) and the remaining *RUNX1* allele is seldom mutated in leukaemic cells of patients, haploinsufficiency of *RUNX1* (*RUNX1*+/- status) is thought to be the basis for leukaemogenesis. These observations suggest that the underlying mechanisms of leukaemogenesis caused by *RUNX1* chimaeric genes and point mutations all derive from a loss-of-function of *RUNX1*.

Extensive studies have revealed that *RUNX* alterations do not readily result in leukaemia. This conclusion was deduced from the following findings: chimaeric genes are detected even in healthy volunteers (Basccke *et al*, 2002; Mori *et al*, 2002), and mouse models carrying various *RUNX* 1 alterations do not develop leukaemia (Rhoades *et al*, 2000; Higuchi *et al*, 2002). Furthermore, the approximately 37% incidence of AML in FPD/AML patients (Song *et al*, 1999; Michaud *et al*, 2002; Osato, 2004) may reflect a requirement for additional genetic

(or epigenetic) alterations, in addition to the *RUNX1*<sup>+/-</sup> status. The identification of such 'second hits' would help to elucidate the mechanisms behind leukaemogenesis.

Retroviral insertional mutagenesis is a potentially powerful tool in identifying additional genetic changes that co-operate with *RUNX* alterations in leukaemogenesis. Ecotropic retroviruses integrate randomly into the host genome, resulting in activation of oncogenes or disruption of tumour suppressor genes (Jonkers & Berns, 1996). Consequently, mice infected by retroviruses develop leukaemia within a relatively short period. The integration site, in turn, can be used as a tag to identify oncogenes or tumour suppressor genes (Suzuki *et al*, 2002). To employ retroviral mutagenesis, it is necessary to inoculate mice with a replication-competent retrovirus or to use specific strains bearing a transmissible virus, such as the murine BXH2 strain. In such mice, retroviral insertion occurs spontaneously and 90% of the animals develop leukaemia within a year (Bedigian *et al*, 1984). Interestingly, BXH2 mice suffer from myeloid leukaemias, whereas most retroviruses induce lymphomas in infected mice. The myeloid features of these mice have been attributed to the BXH2 genetic background because other strains develop lymphoma when they are infected with the BXH2 ecotropic retrovirus (BXH2 retrovirus) by the foster mother method (Bedigian *et al*, 1993). Recently, a locus responsible for these myeloid features was reported to lie in an 18-cM region of chromosome 8 (Turcotte *et al*, 2004).

Many lines of evidence suggest that haploinsufficiency of *RUNX1* is associated with FPD/AML. However, the notion that *RUNX1*<sup>+/-</sup> status *per se* promotes leukaemogenesis remained to be addressed with a solid experimental approach. In this study, we generated BXH2-*Runx1*<sup>+/-</sup> mice, which developed leukaemias earlier than their BXH2-*Runx1*<sup>+/+</sup> littermates (BXH2-*Runx1*<sup>+/+</sup> mice will be referred to as wild type in this communication). Leukaemias that developed in BXH2-*Runx1*<sup>+/-</sup> mice were more myeloid-specific than those induced in wild-type mice. Identification of retroviral integration sites (RIS) revealed that the *c-Kit* gene, frequently mutated in human *RUNX* leukaemias, was recurrently affected in BXH2-*Runx1*<sup>+/-</sup> mice. Therefore, these results suggest that the *Runx1*<sup>+/-</sup> status predisposes mice to myeloid leukaemia and that the murine BXH2-*Runx1*<sup>+/-</sup> system recapitulates FPD/AML.

## Materials and methods

### *Runx1*<sup>+/-</sup> mice

The *Runx1*<sup>+/-</sup> mouse was generated by Okada *et al* (1998) as they previously described. Genotyping of the targeting allele was performed by polymerase chain reaction (PCR) for intron 4 and the PGK promoter of the inserted *neo* gene. *Runx1*<sup>+/-</sup> mice were maintained in the C57BL/6 background. All animal experiments were performed according to the Guide for the Use of Experimental Animals in the Institute of Molecular and Cell Biology.

### Generation of BXH2-*Runx1*<sup>+/-</sup> mice

To carry out retroviral insertional mutagenesis, C57BL/6-*Runx1*<sup>+/-</sup> and BXH2 mice were crossed. As the ecotropic retrovirus in BXH2 is mainly transmissible through milk, male C57BL6-*Runx1*<sup>+/-</sup> mice were crossed with female BXH2 mice. At least three generations of backcrosses were carried out to generate BXH2-*Runx1*<sup>+/-</sup> mice and wild-type littermates.

### Sequencing of the BXH2 retroviral genome

The entire BXH2 retroviral genome was not determined although it is known to share similarity with that of the Akv retrovirus. Hence, two independent proviruses were cloned from distinct integration sites by using genomic sequence-specific primers and long accurate PCR. The sequences of these BXH2 retroviral genomes are available in the DNA Data Bank of Japan database (accession numbers AB213652 and AB213653).

### Haematological analysis

Since inbred BXH2 mice develop leukaemia as early as 7 months, BXH2-*Runx1*<sup>+/-</sup> mice were monitored from 5 months onwards. Full blood counts of peripheral blood (PB) were obtained weekly by an automatic haematology analyser piloted by veterinary software (Celltac alpha MEK-6358; Nihon Kohden, Osaka, Japan). When the white blood cell count increased beyond  $30 \times 10^9/l$ , the mice were carefully observed twice daily. Moribund mice were sacrificed and subjected to necropsy. The following abnormalities in haematopoietic tissues were recorded: enlargement of thymus, liver and spleen, and swelling of lymph nodes. Leukaemic cells from PB, bone marrow (BM) and spleen were subjected to May-Giemsa staining. Immunophenotypic analysis was carried out by flow cytometric analysis using a standard method. Briefly, blocking non-specific binding in 50  $\mu$ l of mouse serum was followed by antibody staining on ice for 1 h. After washing, cells were suspended in 1 ml of phosphate-buffered saline with 2  $\mu$ g/ml of propidium iodide (PI; Sigma, St Louis, MO, USA) for dead cell discrimination. On the screen of flow cytometry (FACS Vantage; Becton Dickinson, San Jose, CA, USA), homogenous population in cell size [forward scatter-side scatter (FSC-SSC) window] and PI-negative viable cells were gated and analysed for individual antigen expressions. All antibodies were purchased from Pharmingen (San Diego, CA, USA): anti-mouse fluorescein isothiocyanate-conjugated c-Kit (2B8), Fas (Jo2), Ter119 (TER-119), CD19 (1D3), Mac1 (M1/70) and phycoerythrin-conjugated Gr-1 (RB6-8C5), CD34 (RAM34), B220 (RA3-6B2), CD61 (2C9.G2), CD4 (H129.19).

### Analysis of immunoglobulin gene rearrangements

Rearrangements of immunoglobulin heavy chain (*IgH*) genes were detected using a previously described PCR method (Hayashi *et al*, 2003; Zeisig *et al*, 2003). Genomic DNA from

leukaemic cells from the spleen was purified and subjected to PCR with ExTaq (Takara Bio, Otsu, Japan) using an initial preheating step at 95°C for 5 min followed by 35 cycles of 95°C for 45 s, 60°C for 40 s and 72°C for 1 min. The primers employed were forward 1 (DJ-F1) (5'-acgtcgactttgts-aaggatctactactgt-3') and reverse (DJ-R) (5'-gggtctagactct-cagccggctcctcaggg-3'). Germline DNA was also amplified with ExTaq using an initial preheating step at 95°C for 5 min followed by 30 cycles of 95°C for 45 s, 58°C for 40 s and 72°C for 1 min. The primers employed were forward 2 (JH1-4) (5'-tgctgtggaacagtacaatcatg-3') and reverse (DJ-R). The murine B-cell lines A20 and 2PK3, established from lymphomas, were used as positive controls.

### Identification of RIS by inverse PCR

The inverse PCR method was carried out as previously described (Yanagida *et al*, 2005). Briefly, 5 µg of genomic DNA extracted from BXH2 leukaemic cells from the spleen was digested by *Bst*YI and self-circularised. Then, 5'- and 3'-integration flanking fragments were individually amplified by inverse PCR, cloned by the TA cloning vector and sequenced. RIS were mapped by a BLAST-like alignment tool search of the UCSC Genome Bioinformatics database (<http://genome.ucsc.edu>). Common integration sites (CIS) were similarly defined using the retroviral-tagged cancer gene database (RTCGD) (<http://RTCGD.ncicrf.gov>); window sizes were 100, 50 and 30 kb for CIS with four or more, three or two insertions, respectively, in each model (Akagi *et al*, 2004).

### Southern analysis of RIS

To determine whether the leukaemic clone with a particular integration site is a major or a minor clone in the mouse and to identify 'masked cases' of a particular integration site, Southern blotting was performed in a standard procedure using random-primed [<sup>32</sup>P] dCTP labelling. Ten microgram of genomic DNA extracted from BXH2 leukaemic cells from the spleen was digested by *Bam*HI, *Eco*RI or *Pvu*II. The genomic DNA probe for the *c-Kit* locus was the 486-bp *Bst*YI-*Stu*I fragment in the vicinity of the integration site in leukaemia 292, another BXH2 model that bears a *Runx1* alteration.

### Retroviral vector

Human *c-KIT* cDNA from R. J. Arceci (Johns Hopkins Oncology Center) was inserted into the retroviral vector MIG [MSCV/Internal ribosomal entry site (IRES)/ green fluorescent protein (GFP)] (DeKoter *et al*, 1998).

### Packaging cell-line cultivation and retrovirus supernatant preparation

After 1 week of selection with diphtheria toxin and hygromycin, approximately  $2 \times 10^7$  cells were transfected with 120 µg

plasmid DNA with the CellPfect Transfection Kit (Amersham Biosciences, Piscataway, NJ, USA). Supernatants were collected 24 and 48 h after transfection and centrifuged at 7500 g at 4°C overnight. The pellet containing the retrovirus was resuspended with 1.5 ml of  $\alpha$ -minimum essential medium ( $\alpha$ -MEM; Gibco, Carlsbad, CA, USA) and stored at -80°C. The viral titre was calculated with NIH3T3 cells to be  $>10^6$  colony-forming units (CFU)/ml.

### Infection of BM cells with recombinant retrovirus

Eight weeks old wild-type or *Runx1*<sup>+/-</sup> C57BL/6 mice were injected intraperitoneally with 2.5 mg of 5-fluorouracil (5-FU; Sigma). Five days after injection, BM cells were collected from tibias and femurs, and  $10^6$  BM cells were precultured 1 d in a 6-well plate with 2 ml of  $\alpha$ -MEM supplemented with 10% fetal bovine serum, 10 ng/ml of recombinant mouse interleukin 3 (IL-3; R&D systems, Minneapolis, MN, USA), recombinant mouse (experiment 1) or human (experiment 2) stem cell factor (SCF; PeproTech, Rocky Hill, NJ, USA), 100 ng/ml of recombinant mouse granulocyte colony-stimulating factor (G-CSF; PeproTech), 5 ng/ml of recombinant mouse erythropoietin (EPO; Pharmingen) and antibiotics at 37°C with 5% CO<sub>2</sub>. The cells were then mixed with 500 µl of retrovirus-containing medium and 50 µg RetroNectin (Takara Bio) and centrifuged at 780 g at 30°C for 1.5 h (spin infection). Another 500 µl of retrovirus-containing medium was spin-infected the next day. After culture for several days, EGFP-positive cells were sorted with a FACS Vantage (Becton Dickinson, Heidelberg, Germany). The expression of human *c-KIT* gene introduced by the retroviral vector was confirmed by reverse transcription PCR using 32Dcl3 cells. Primers employed are as follows; 5'-gacgagttggcctaga-3' and 5'-gaggggtgacccaacactgat-3'.

### Colony-forming unit-culture (CFU-C) assay

EGFP-positive sorted cells ( $10^4$ ) were cultured in 35-mm dishes in triplicate in Methocult M3231 methylcellulose medium (StemCell Tec., Vancouver, BC, Canada) supplemented with 20 ng recombinant mouse IL-3, mouse (experiment 1) or human (experiment 2) SCF, 200 ng mouse G-CSF and 10 ng mouse EPO. Colonies were counted on day 10. In experiment 1, 3000 cells from primary colonies were replated in triplicate and secondary colonies were counted after 10 d.

### Mutational analysis of *c-KIT* and *FLT3* in human leukaemias

Twenty-five human leukaemia patients belonging to the following categories were screened for mutations in the *c-KIT* and *FLT3* genes: t(8;21) ( $n = 9$ ), inv(16) ( $n = 10$ ), and *RUNX1* point mutation ( $n = 6$ ). An analysis of *c-KIT* and *FLT3* mutations for nine patients with t(8;21) AML and three patients with AML M0 harbouring a *RUNX1* mutation was previously reported (Matsuno *et al*, 2003). Each patient gave

informed consent to this study according to the guidelines based on the tenets of the revised Helsinki protocol produced by the Institutional Committees for the Protection of Human Subjects and Analysis of the Human Genome. Mononuclear cells were isolated from PB or BM samples at the time of diagnosis by Ficoll–Conray density gradient centrifugation. Total cellular RNA was extracted by ultracentrifugation in a guanidium-isothiocyanate/CsCl<sub>2</sub> gradient or TRIzol reagent (Gibco BRL, Gaithersburg, MD, USA). cDNA was synthesised from total RNA and the oligo (dT)<sub>12–18</sub> primer with SuperScript II reverse transcriptase (Invitrogen Life Technologies, Carlsbad, CA, USA). Exon 8 and the tyrosine kinase domain 2 (TK2) of *c-KIT* and the juxtamembrane region (JM) and TK2 of *FLT3* were sequenced with the following primers: 5′-ccctgttactctcttct-3′ and 5′-gggacaacataagaact-3′ for *c-KIT* exon 8, 5′-tgtattcacagacttg-3′ and 5′-cgacagaattgatccgcacag-3′ for *c-KIT* TK2, 5′-catccaagacaacatctc-3′ and 5′-ccagcc-tttttgttttc-3′ for *FLT3* JM, and 5′-ccccactttccaactca-3′ and 5′-ggataggtggaggatgaa-3′ for *FLT3* TK2. A total of 100 µl of each amplified product was purified and directly sequenced in both directions with the BigDye Terminator Cycle Sequencing Ready Reaction kit (Applied Biosystems, Foster City, CA, USA). Products bearing mutations were subcloned into the vector pGEM-T (Promega, Madison, WI, USA) and subjected to cycle sequencing. Restriction fragment length polymorphism (RFLP) analysis was performed to confirm alterations. For RFLP analysis, amplified fragments of the TK2 moieties from *c-KIT* and *FLT3* were cleaved with *Alw26I* and *EcoRV* respectively.

### Statistical analysis

The survival curves of BXH2-*Runx1*<sup>+/-</sup> and wild-type control mice were compared by using the Kaplan–Meier method and differences were calculated by the Mantel–Cox test. Differences in the immunophenotypic and morphological parameters of BXH2-*Runx1*<sup>+/-</sup> and wild-type leukaemias were analysed with the *F*-test. The numbers of colonies were compared by the analysis of variance (ANOVA) with *post hoc* test.

## Results

### *BXH2-Runx1*<sup>+/-</sup> mice develop myeloid leukaemia with a shorter latency period than that of wild-type littermates

As the *Runx1*<sup>+/-</sup> mouse is genetically equivalent to human FPD subjects, we first studied *Runx1*<sup>+/-</sup> mice of the C57BL/6 background. These mice did not show any apparent haematological defects except for previously described phenotypes: decreased numbers of CD4<sup>+</sup> lymphocytes (Hayashi *et al*, 2000) and a mild decrease in platelets (Sun & Downing, 2004). They also did not develop spontaneous leukaemia. Thus, we used the retroviral mutagenesis approach to induce leukaemia in BXH2 mice. The survival curves obtained from generations N3–N10 of 36 BXH2-*Runx1*<sup>+/-</sup> mice and 44 wild-type

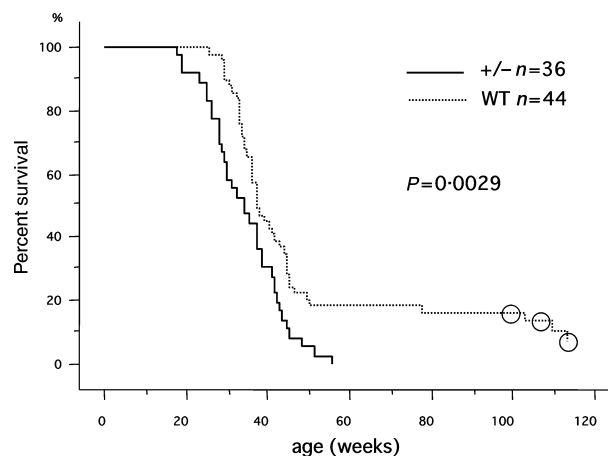


Fig 1. Decreased disease latency in BXH2-*Runx1*<sup>+/-</sup> mice. The percentage of mice surviving *versus* age in weeks was plotted for BXH2-*Runx1*<sup>+/-</sup> mice (+/-, solid line, *n* = 36) and wild-type littermates (WT, dotted line, *n* = 44). The *Runx1*<sup>+/-</sup> mice showed earlier disease onset (mean: 34.4 vs. 50.2 weeks) and higher incidence (100% vs. *c.* 85% at 12 months). The Kaplan–Meier method indicated the survival of the two groups differed significantly (*P* = 0.0029, Mantel–Cox test). Open circles represent censored cases.

littermates clearly showed that the *Runx1*<sup>+/-</sup> mice had a decreased disease latency (mean: 34.4 weeks vs. 50.2 weeks) and a higher disease incidence (100% vs. *c.* 85% at 12 months) (*P* = 0.0029, Mantel–Cox test; Fig 1), suggesting that *Runx1* haploinsufficiency augments leukaemia formation.

### *BXH2-Runx1*<sup>+/-</sup> mice show stronger myeloid features than control littermates

Leukaemic cells from the BM (Fig 2A), PB (Fig 2B) and spleen (data not shown) of BXH2 mice predominantly exhibited immature myeloid features, a result that was confirmed by immunophenotypic analysis by flow cytometry (Table I). In addition, leukaemic cells from a substantial number of BXH2 mice also had monoblastic and lymphocytic features (Fig 2C and D and Table I). A mature fraction of myeloid cells (polynuclear cells) was observed in some cases (Fig 2E and Table I). In all BM samples, macrophages or pseudo-Gaucher histiocytes were found, as reported (Kogan *et al*, 2002) (Fig 2A). In all cases, BXH2 leukaemic cells were positive for the myeloid antigens Gr-1 and Mac1. They were also frequently positive for immature antigens, such as *c-Kit* and Fas. Surprisingly, flow cytometric analysis showed that three of nine wild-type BXH2 leukaemic cell samples were positive for B220, a B-cell marker. Two-colour staining indicated that B220<sup>+</sup> cells were simultaneously positive for the Mac1 antigen (Fig 2F). However, these cells were completely negative for another B-cell marker, CD19. Hence, a substantial fraction of BXH2 leukaemias in wild-type controls seem to show B220<sup>+</sup> CD19<sup>-</sup> B-cell features. In contrast, only one of 10 BXH2-*Runx1*<sup>+/-</sup> leukaemias was positive for B220. B220 positivity in BXH2-*Runx1*<sup>+/-</sup> leukaemias was significantly less frequent



**Table I.** Fluorescence-activated cell sorting analysis and haematological data of BXH2 leukaemias.

No.†	Genotype	c-Kit (%)	Gr-1 (%)	Fas (%)	CD34 (%)	Mac1 (%)	B220 (%)	Ter119 (%)	CD61 (%)	CD19 (%)	CD4 (%)	WBC (10 <sup>9</sup> /l)	Sp (mg)	PNC (%)‡	Mono (%)‡	J <sub>H</sub> §
004	+/-	89	57	67	2	97	3	5	4	1	0	65	352	<u>21.4</u>	8.9	G/G
008	+/-	46	37	22	0	88	NA	1	16	NA	NA	34	500	4.0	9.7	G/G
036	+/-	1	65	9	1	84	4	1	1	2	0	451	538	<u>56.6</u>	6.5	G/G
042	+/-	3	54	36	2	79	<u>26</u>	4	14	3	1	118	670	0.8	35.1	G/G
069	+/-	16	70	36	10	88	10	NA	3	1	NA	311	575	2.4	1.2	G/G
098	+/-	11	80	43	7	96	6	4	29	4	2	124	601	<u>44.7</u>	0	G/G
115	+/-	30	65	47	5	76	8	5	13	2	1	142	572	<u>21.8</u>	47.2	G/G
118	+/-	28	87	53	5	91	2	3	19	2	2	91	486	<u>78.8</u>	19.2	G/G
182	+/-	19	69	34	9	84	8	6	33	3	3	77	780	<u>28.6</u>	0	G/G
243	+/-	NA	NA	38	1	88	6	6	5	4	0	88	632	<u>30.9</u>	7.4	G/G
003	WT	47	74	21	14	88	<u>37</u>	3	9	2	3	NA	620	0.8	28.8	G/G
006	WT	1	24	6	0	70	3	2	0	2	0	95	552	<u>29.1</u>	17.2	G/G
041	WT	2	22	68	0	95	3	1	5	2	0	NA	441	15.5	0.9	R/G
067	WT	20	59	19	3	80	4	2	10	1	0	317	850	13.6	10	G/G
068	WT	9	68	15	9	94	<u>50</u>	1	10	1	1	305	288	3.4	3.4	G/G
099	WT	10	84	17	10	90	2	2	8	2	3	123	615	11.3	0	G/G
117	WT	31	75	34	3	84	<u>21</u>	3	24	6	1	NA	375	12.7	0	G/G
181	WT	34	61	37	7	94	4	9	18	5	1	221	745	12.6	1.9	R/G
242	WT	17	84	19	1	72	1	1	12	2	0	84	677	<u>36.7</u>	0	G/G
Mean	+/-	27	65	39	4	87	8*	4	14	2	1	150	571	29.0**	13.5	
	WT	19	61	26	5	85	14	3	11	3	1	191	574	15.1	6.9	

PB or BM cells were analysed. The underlined cases are positive for indicated categories.

WT, wild type; NA, not available; WBC, white blood cell; Sp, spleen; PNC, polynuclear and ring-form cells; PB, peripheral blood; G, germ line; R, rearranged.

\* $P = 0.00550$ , \*\* $P = 0.01239$  ( $F$ -test).

†Mouse identification number.

‡Percentage of polynuclear (PNC) and ring-shaped cells and cells with obvious monocytic components in the PB.

§J<sub>H</sub> status (see Fig 2G).

and *HoxA7/A9* loci did not seem to be specific to BXH2-*Runx1*<sup>+/-</sup> leukaemias. On the contrary, the *c-Kit* locus was affected twice among 24 BXH2-*Runx1*<sup>+/-</sup> mice but was not involved in any of our 17 BXH2 wild-type mice or in the 135 inbred BXH2 mice in the RCGD database (Table II, highlighted in bold). Southern blotting suggests that cells with a retroviral insertion at the *c-kit* locus constituted the major clone in the BXH2-*Runx1*<sup>+/-</sup> leukaemia of mouse 004 (Fig 3C), and the integration site was approximately 120-kb downstream of the *c-Kit* gene. This distance is thought to be close enough to result in the overexpression of target genes (Jonkers & Berns, 1996). Indeed, flow cytometric analysis revealed that leukaemic cells from mouse 004 showed an exceptionally high frequency of c-Kit positivity (Fig 3D). In the other case of *c-kit* integration, mouse 005, the retrovirus had integrated approximately 20-kb upstream of the *c-Kit* gene with the same orientation. Hence, this viral insertion should result in the overexpression of *c-Kit*, but we were unable to confirm this due to death of the mouse and therefore only DNA was available for analysis.

Three to five simultaneous integrations usually take place in BXH2 leukaemias. The RIS concurrently observed within a

single leukaemia are summarised in 'Interactive Search' in the RCGD database. Currently, eight integrations into *Evi-13* (*Runx1*) locus are listed in RCGD. The coinciding RIS are shown in the right hand most column of Table II. Of these, two of the eight *Runx1*-integrated tumours showed simultaneous integrations in the *c-kit* locus. Therefore, the activation of *c-KIT* may co-operate with *RUNX1*<sup>+/-</sup> or other *RUNX*-related alterations in leukaemogenesis.

#### *Overexpression of c-KIT co-operates with Runx1+/- status in a colony-forming assay*

To confirm the co-operative role of *Runx1*<sup>+/-</sup> and overexpression of *c-Kit*, we introduced the human *c-KIT* gene into BM cells from C57BL/6-*Runx1*<sup>+/-</sup> or C57BL/6 wild-type mice using a retroviral vector. IRES-driven *EGFP* gene in the MIG retrovirus vector allows sorting of infected cells (Fig 4A and B). Using only sorted *EGFP*-positive cells, we carried out a CFU-culture (CFU-C) assay of BM cells in the presence of mouse SCF but we did not detect any significant difference in colony numbers (data not shown). Next we replated haematopoietic cells from primary colonies. *Runx1*<sup>+/-</sup> cells expres-

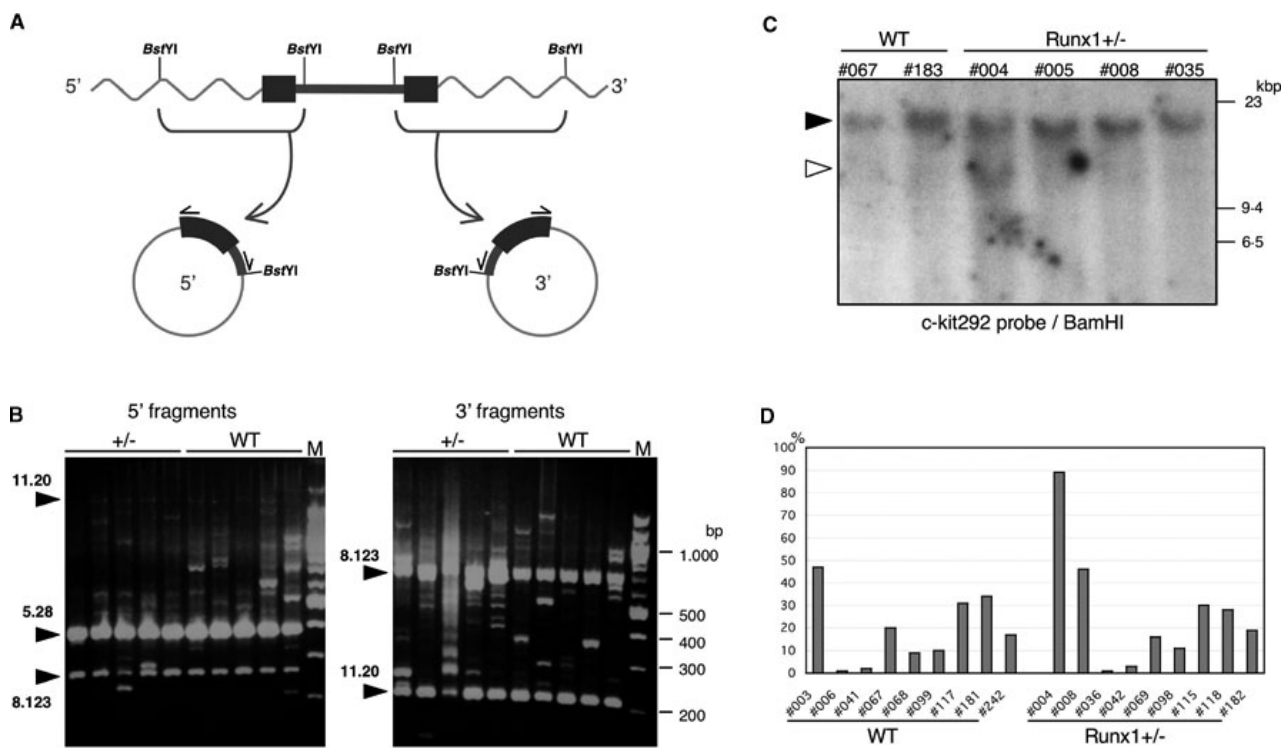


**Fig 3.** Inverse polymerase chain reaction (PCR) analysis of leukaemic cells and *c-Kit* expression of the integrated cases. (A) Schematic depiction of the inverse PCR method. Sequences flanking the 5'- and 3'-sites of integration were digested by *Bst*YI, self-ligated and amplified separately. (B) Inverse PCR of leukaemic cells. The arrowheads depict the three germline-specific bands and are labelled with their corresponding location on the mouse chromosome (chromosome number followed by a dot and the position, in Mb). Several additional bands were amplified from the somatically acquired integrations in each leukaemic cell sample. M, molecular marker. (C) Southern blot hybridisation with the *c-kit292* probe. The closed arrowhead depicts germline bands while the open arrowhead depicts a rearranged band. (D) Frequency of *c-Kit* positivity in leukaemic cells from wild type and *BXH2-Runx1*<sup>+/-</sup> mice, as determined by flow cytometric analysis (Table 1).

sing *c-KIT* produced significantly higher numbers of secondary colonies than other transfectants (experiment 1, Fig 4D). To minimise the effect of supplemented mouse SCF, which can activate endogenous mouse *c-Kit* expressed in BM cells, we next carried out the CFU-C assay using human SCF, which has little effect against mouse *c-Kit* (experiment 2, Fig 4E). Interestingly, even in a primary CFU-C assay, *c-KIT* transfectants gave rise to higher number of colonies than controls, regardless of whether they were derived from C57BL/6 wild-type or *Runx1*<sup>+/-</sup> BM cells. In addition, *Runx1*<sup>+/-</sup> cells expressing *c-KIT* formed higher number of colonies than wild-type cells expressing *c-KIT*. Taken together, the *Runx1*<sup>+/-</sup> status and overexpression of *c-Kit* appear to act synergistically with respect to stimulating the proliferation of haematopoietic progenitor cells.

*Constitutively active mutations of the c-KIT and FLT3 genes occur frequently in human RUNX leukaemias*

To determine whether upregulation of *c-KIT* co-operates with *RUNX1* deficiency in human leukaemogenesis, as suggested by the mouse system, human leukaemia samples bearing *RUNX* alterations, a *RUNX1* point mutation or the t(8;21) or inv(16)

rearrangements were screened for mutations in *c-KIT*. In addition, mutations in *FLT3* were sought as *c-KIT* and *FLT3* share structural properties and are classified as type III receptor tyrosine kinases (RTK) (Scheijen & Griffin, 2002). They also function in the same signalling cascades, including the RAS and the phosphatidylinositol-3-kinase pathways (Scheijen & Griffin, 2002). Thus, *c-KIT* and *FLT3* are considered to be functionally equivalent in the regulation of cell proliferation, although they have distinct activities. Three t(8;21) leukaemias showed mutations in the *c-KIT* TK2 region: two mutations affected the D816 residue (substitution with V or E) and one N822K mutation (Fig 5A). Several of the leukaemias also showed mutations in the JM and TK2 regions of *FLT3*. Five patients, one with t(8;21) leukaemia and the other four bearing *RUNX1* point mutations, had internal tandem duplication (ITD) mutations in the JM region of *FLT3*. Direct sequencing of the amplified PCR products showed overlapping patterns of the wild-type and mutant genes (Fig 5B). Moreover, the *FLT3* residue D835, which is equivalent to the *c-KIT* residue D816, was mutated in two leukaemias, one with the inv(16) translocation and the other with a *RUNX1* point mutation. These mutations resulted in D835Y and D835E substitutions respectively (Fig 5C). We

**Table II.** Retroviral integration sites identified by inverse polymerase chain reaction and Southern blotting.

	Chromosome position [chromosome (Mb)]†	RIS/gene*	Hits in this study		Hits in RTCGD		RUNX1 concurrent‡
			+/-	WT	BXH2	All	
Number of tumours			24	17	135	927	8
Known CIS (27)§	11-8	Nf-1 (Evi-2)	3	2	9	14	0
	6-52	HoxA7/A9	3	0	9	13	0
	11-18	Meis1	1	0	10	15	0
	13-28	Evi-15,16 (Sox4)	1	0	9	63	0
	10-20	Myb	1	0	6	45	1
	12-99	Evi-151 (4831426119Rik)	1	0	2	3	0
	5-137	Evi-165 (Mafk)	0	1	2	2	0
	13-93	Evi-19 (Hmgcr)	0	1	2	2	0
	17-28	Pim1	0	1	2	31	0
	5-75	<b>c-kit/Kdr</b>	<b>2</b>	<b>0</b>	<b>0</b>	<b>9</b>	<b>2</b>
	1-13	Evi-32 (Ncoa2)	1	0	0	3	0
	1-86	Ptma	1	0	1	3	0
	2-105	Lmo2	1	0	0	2	0
	<b>2-118</b>	<b>Evi-18 (RasGrp1)</b>	<b>1</b>	<b>0</b>	<b>1</b>	<b>24</b>	<b>1</b>
	2-145	Evi-46 (Snx5)	1	0	1	3	0
	4-132	Cd52	1	1	0	2	0
	4-133	Evi-11 (Cnr2)	1	0	0	6	0
	5-110	Evi-65 (Selp1)	1	0	0	3	0
	7-99	Mrvi1	1	0	1	3	0
	11-24	Evi-9 (Bcl11A)	1	1	1	7	0
	13-23	Hist1h1c	1	1	1	3	0
	13-27	Casvis12	1	0	0	1	0
	15-73	Dkmi21 (Ptp4a3)	1	0	0	3	0
	16-92	Evi-160 (Ifngr2)	1	0	1	2	0
	2-46	Nki3 (Zfhx1b)	0	1	0	11	1
	14-20	Evi-26 (Rai17)	0	1	1	3	0
	18-14	Evi-3	0	1	1	6	0
RIS-1 (3)§	14-42	Slis-2	0	1 (1)¶	0	0	0
	16-94	Slis-3	0	2 (1)¶	0	0	0
	Un	Slis-4	1	1 (3)¶	0	0	0
RIS-2 (19)§	1-134	Myog	1	0	0	1	0
	3-116	Edg1	1	0	1	1	0
	4-130	Rpa2	1	0	0	1	0
	5-122	Ubc	1	0	0	1	0
	7-116	Itgax	1	0	0	1	0
	8-40	Pdgrf1/Atip1-pending	1	0	0	1	0
	8-69	Mef2b	1	0	0	1	0
	8-69	Lsm4	1	0	0	1	0
	9-108	6330580J24Rik	1	0	0	1	0
	11-69	F730038F15Rik	1	0	0	1	0
	11-83	Sfn2	1	0	0	1	0
	11-95	Ppp1r9b	1	0	0	1	0
	11-121	2900052L18Rik	1	0	0	2	0
	12-74	Zfp361	1	0	0	1	0
	18-34	Pkd2l2	1	0	0	1	0
	18-38	0610009O20Rik	1	0	0	1	0
	X.11	Ddx3x	1	0	0	1	0
	1-135	C920001D21Rik/Ptprv	0	1	0	2	0
	15-82	Tob2	0	1	0	1	0
Single RIS (100)	-	-	57	43	0	0	0
Total (149 RIS)	161 Tags		101	60	300	3160	

RTCGD, retroviral-tagged cancer gene database; +/-, BXH2-Runx1 +/- mice; WT, wild-type BXH2 littermate controls; CIS, common integration site; RIS, retroviral integration site; Slis, Singapore leukaemia integration site.

\*RIS or candidate genes in the vicinity of the RIS are shown. The underlined genes/RISs represent those whose coding sequence is disrupted.

†The genomic positions of each RIS was determined by a BLAST-like alignment tool search of the UCSC Genome Bioinformatics database. The chromosome number is followed by a dot and the position in megabases (Mb).

‡Eight tumours in the RTCGD contained insertions upstream of *Runx1*. The number of tumours with concurrent integrations at the listed sites are noted.

§The total numbers of CIS or RIS in each category are indicated in parentheses.

¶Other integrations into Slis were identified in a study of BXH2 mice with another Runx1 abnormality (Yanagida *et al*, 2005).

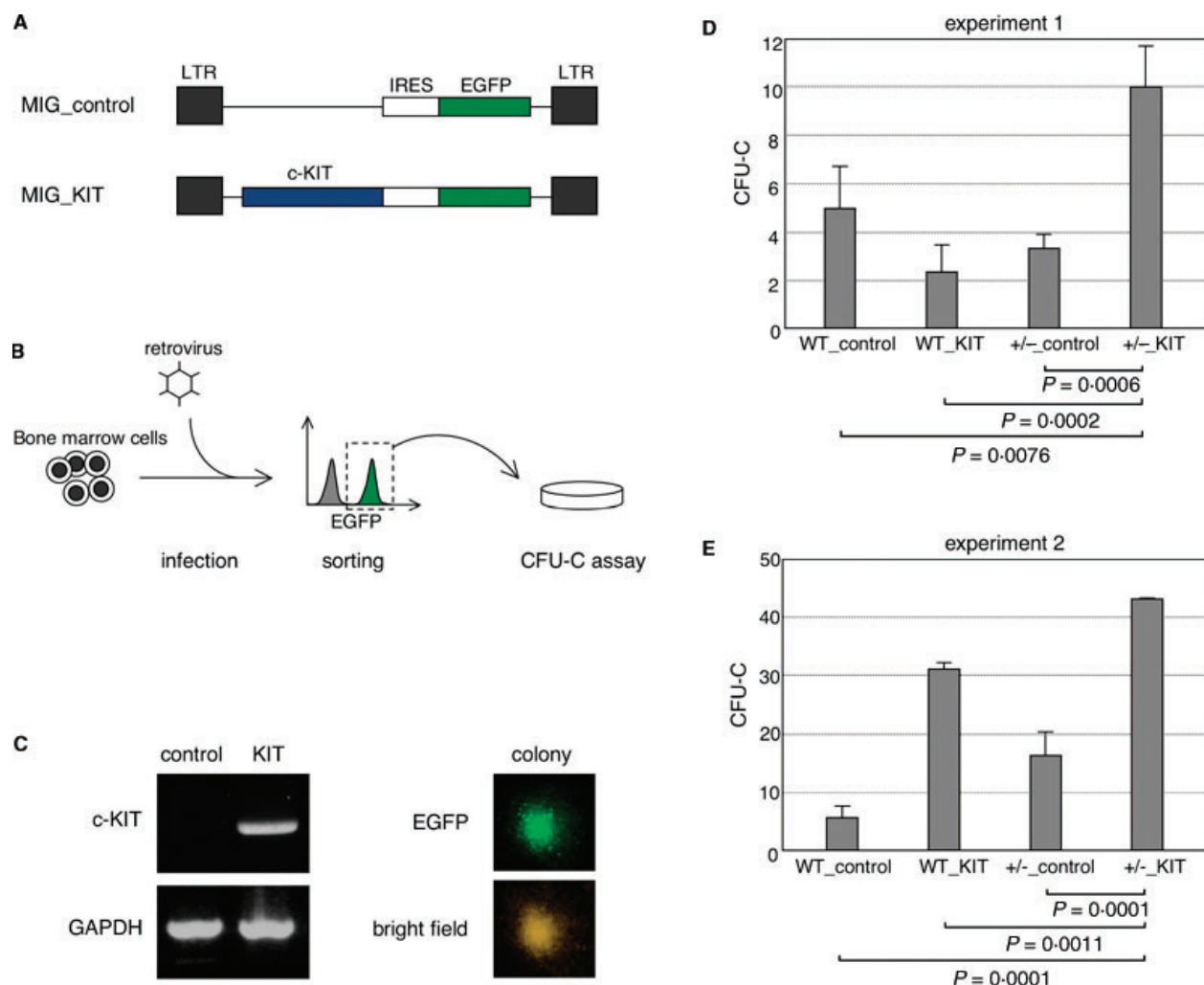


**Fig 4.** Co-operative stimulation of proliferation of haematopoietic progenitor cells by the *Runx1*<sup>+/-</sup> status and *c-KIT* overexpression. (A) Structures of retroviral constructs for control (MIG-control) or *c-KIT* (MIG-KIT) expression. The human *c-KIT* gene was inserted into the indicated position of the plasmid MIG with an Internal ribosome entry site (IRES) and the enhanced green fluorescent protein (*EGFP*) gene. (B) Schematic depiction of the colony-forming unit culture (CFU-C) assay. 5-Fluorouracil treated bone marrow cells were infected with retrovirus vector carrying *c-KIT* and *EGFP* genes, and *EGFP* positive cells were sorted and subjected to the CFU-C assay. The expression of human *c-KIT* gene was confirmed by reverse transcription-polymerase chain reaction (C, left) in 32Dcl3 cells. Glyceraldehyde-3-phosphate dehydrogenase (GAPDH) served as an internal control. All colonies expressed *EGFP* (C, right). The numbers of secondary CFU-C per  $3 \times 10^3$  cells (D, experiment 1) or primary CFU-C per  $10^4$  cells (E, experiment 2) are shown. Each transfectant was cultured in triplicate and averages and standard deviations are indicated. Statistical differences in ANOVA with *post hoc* test are shown at the bottom. *Runx1*<sup>+/-</sup> bone marrow cells transfected with the *c-KIT* gene give rise to higher numbers of colonies than other transfectants.

confirmed the presence of the *c-KIT* D816 and *FLT3* D835 mutations by RFLP analysis, which showed that two t(8;21) patients (549 and 552) had a mutation affecting the *Alw26I* site in the *c-KIT* TK2 region (Fig 5D), and that *FLT3* TK2 was mutated in the *EcoRV* site in patients 37 and 462, who have the inv(16) translocation and a *RUNX1* point mutation respectively (Fig 5E). Although 24–50% of inv(16) cases are reported to carry mutations in *c-KIT* exon 8 (Gari *et al*, 1999), none of our patients had this mutation. Altogether, 10 of 25 (40%) of our human leukaemia cases bearing *RUNX* abnormalities had *c-KIT* or functionally equivalent *FLT3* mutations (Table III).

## Discussion

To determine whether the *RUNX1*<sup>+/-</sup> status *per se* contributes to leukaemogenesis, we investigated the effect of monoallelic inactivation of *Runx1* in a myeloid leukaemia-prone mouse strain, BXH2. BXH2-*Runx1*<sup>+/-</sup> mice showed a decreased disease latency and a higher incidence of leukaemia compared with their wild-type littermate controls. In addition, BXH2-*Runx1*<sup>+/-</sup> leukaemias showed stronger myeloid features than BXH2 leukaemias. Wild-type BXH2 leukaemias were myeloid leukaemias with substantial B-cell features, while BXH2-*Runx1*<sup>+/-</sup> leukaemias showed far fewer B-cell characteristics

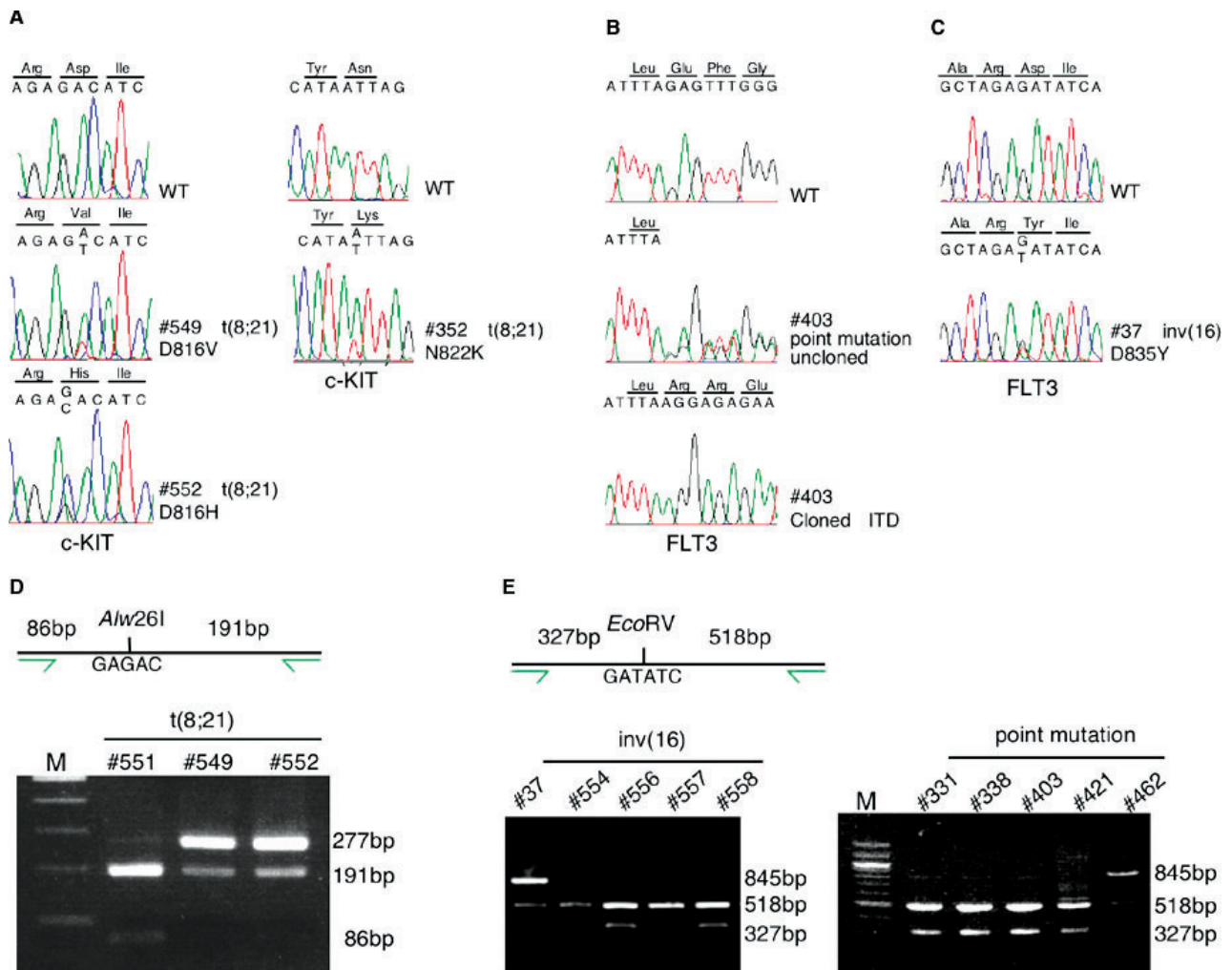


**Fig 5.** Mutations of *c-KIT* and *FLT3* in human leukaemias. (A) Sequences of the *c-KIT* D816 (left) and *c-KIT* N822K (right) mutations in leukaemias with t(8;21). The A2447 residue of patient 549 and the C2448 residue of patient 552 are mutated to T and G respectively. These mutations result in amino acid changes of D816 to V and H respectively. The right column shows the complementary sequence that reveals that the T2466 residue of patient 352 is mutated to A, resulting in the N822K mutation. (B) Representative sequences of *FLT3* internal tandem duplication (ITD) mutations in leukaemias that bear a point mutation in *RUNX1*. Top panel, the wild-type cDNA sequence. Middle panel, direct sequence of the mutation. Overlapping sequences from both wild type and the ITD are present. Bottom panel, the TA-cloned sequence of the ITD. (C) Sequences of the *FLT3* D835Y mutation found in inv(16) leukaemias. The G2503 residue of patient 37 is mutated to T. (D) Restriction fragment length polymorphism (RFLP) analysis of the *c-KIT* D816 mutations in leukaemias with t(8;21). Amplified wild-type 277-bp fragments are cleaved into 191- and 86-bp by *Alw261*, whereas mutant fragments are not cleaved. (E) RFLP analysis of the *FLT3* D835 mutations in leukaemias with inv(16) or a *RUNX1* point mutation. The mutant fragments were not cleaved while the amplified wild-type 845-bp fragments were cleaved into 518- and 327-bp fragments by *EcoRV*. M, molecular size marker.

**Table III.** Mutations of *c-KIT* and *FLT3* in human leukemias.

Leukemia subtype	<i>c-KIT</i>		<i>FLT3</i>		Total (%)
	Exon 8	TK2	ITD	TK2	
t(8;21)	0	3	1	0	4/9 (44)
inv(16)	0	0	0	1	1/10 (10)
<i>RUNX1</i> point mutation	0	0	4	1	5/6 (83)
Total	0	3	5	2	10/25 (40)

ITD, internal tandem duplication; TK2, tyrosine kinase domain.

than wild-type BXH2 leukaemias. As even the myeloid tropic retrovirus Gr-1.4 causes B220<sup>+</sup> myeloid leukaemias (Erkeland *et al*, 2004), it appears that myeloid leukaemias arising from retroviral mutagenesis tend to show B-cell features. Therefore, our observation concerning BXH2-*Runx1*<sup>+/-</sup> leukaemias is notable. The stronger myeloid features of BXH2-*Runx1*<sup>+/-</sup> mice are supported by morphological analysis and by the absence of *IgH* gene rearrangement (Fig 2 and Table I).

Retroviral integration into the *c-kit* locus occurred twice among BXH2-*Runx1*<sup>+/-</sup> mice, but not in their wild-type littermates or in 135 BXH2 tumours in the RTCGD database

(Table II, highlighted in bold). An interactive search of the RCGD database revealed that two of eight cases bearing *Evi-13* (*Runx1*) insertions also had a concurrent *c-kit* integration. Overexpression of *c-KIT* exhibited synergy with the *Runx1*<sup>+/-</sup> status in stimulating the proliferation of haematopoietic progenitor cells, as shown by the CFU-C assay. The contribution of *c-KIT* mutations to leukaemogenesis was confirmed by analysis of human leukaemia samples with RUNX alterations. These results suggest that *c-kit* is a preferred 'second hit' site. Furthermore, we also detected an integration into the *Evi-18* locus (*RasGrp1*), which can activate Ras in BXH2-*Runx1*<sup>+/-</sup> mice, but not in wild-type littermates (Table II, highlighted in bold). An interactive search of the RCGD database showed one hit in *RasGrp1* in eight mice that had an integration in *Runx1*. Therefore, *RasGrp1* is also a good candidate for a gene that co-operates with RUNX alterations in leukaemogenesis. As *c-Kit* transmits signals through the Ras pathway, integration into *RasGrp1* may have the same pathological consequences. Together, these observations suggest that *c-Kit* and the Ras pathway co-operate with *Runx1* alterations in murine leukaemogenesis and that the BXH2-*Runx1*<sup>+/-</sup> system recapitulates the leukaemogenesis of FPD/AML.

Why does haploinsufficiency of RUNX1 lead to myeloid leukaemia? A detailed study of *Runx1*<sup>+/-</sup> mice revealed that monoallelic inactivation of *Runx1* results in an increase of haematopoietic progenitor cells, whereas no obvious abnormality is observed in myeloid cell differentiation (Sun & Downing, 2004). This phenotype was further confirmed in conditional *Runx1* knockout mice (Ichikawa *et al*, 2004). The induced expression in murine BM cells of the *RUNX1-ETO* chimaeric gene, which dominantly suppresses RUNX1 function, by the knock-in or transgene strategy also confers a similar increase in primitive progenitor cells, suggesting a higher proliferative property (Rhoades *et al*, 2000; Higuchi *et al*, 2002). In addition, this increase has been shown to be associated with an enhanced self-renewal or immortalisation activity of progenitor cells. Therefore, loss-of-function of RUNX1 is likely to result in an expansion of immature haematopoietic cells with a prolonged life span, thereby providing a time window sufficient for sequential genetic alterations. Although the *RUNX1*<sup>+/-</sup> status seems to have a modest effect on progenitor cells, RUNX1 function is considered to be sufficiently disrupted in the *RUNX1*<sup>+/-</sup> background to create a leukaemogenic potential similar to that conferred by the *RUNX1*<sup>-/-</sup> status or by *RUNX1* chimaeric genes.

In RUNX leukaemias, the incidence of RTK mutations was believed to be low because a number of studies showed that the first identified and most frequent RTK mutation, the FLT3 ITD mutation, occurs only rarely in t(8;21) and inv(16) leukaemias (Thiede *et al*, 2002). However, our retroviral mutagenesis analysis of BXH2-*Runx1*<sup>+/-</sup> mice suggested that *c-Kit* overexpression co-operates with *Runx1* alterations to induce leukaemia. This prompted us to re-evaluate mutations in the *c-KIT* and *FLT3* genes with methods that covered wider regions of the molecules; we also subjected a wider set of

RUNX leukaemias to these analyses so that leukaemias with *Runx1* point mutations were included in addition to the previously studied t(8;21) and inv(16) leukaemias. The results clearly showed that concurrent mutations of RTK genes occur with a high frequency in RUNX leukaemias. Therefore, the BXH2-*Runx1*<sup>+/-</sup> mouse appears useful for identifying unknown 'second hit' loci and hence may help to elucidate the overall mechanism of leukaemogenesis in FPD/AML. Moreover, as loss-of-function of *RUNX1* is a common underlying mechanism in RUNX leukaemias, which include those associated with t(8;21) or inv(16) rearrangements and *RUNX1* point mutations, BXH2-*Runx1*<sup>+/-</sup> mice may be useful for elucidating mechanistic bases not only for *RUNX1*<sup>+/-</sup> leukaemias but also for those characterised by t(8;21) or inv(16) rearrangements.

We assume that additional genetic alterations are essential for the full-blown development of all types of leukaemias. Hence, these 'second hits' should be sought extensively. Unlike what is observed for solid tumours, it is noteworthy that mutations in well-known tumour suppressors, such as p53 and Rb, are rarely found in leukaemia (Imamura *et al*, 1994; Hangaishi *et al*, 1996). Therefore, it is likely that key leukaemia genes remain to be determined. To our knowledge, BXH2-*Runx1*<sup>+/-</sup> is the most myeloid-specific mouse model that is currently available. We believe this model will be very useful for extensive hunts for myeloid leukaemia-specific genes in the future. Analyses of such genes are likely to provide deeper insights into the mechanisms underlying leukaemogenesis.

## Acknowledgements

We thank G. M. Cottles, Y. Saiki, M. Y. Lin, Q. R. Gwee, M. Y. Tan and B. Jacob for technical assistance, R. J. Arceci for *c-KIT* cDNA and G. P. Nolan for Phoenix-Eco cell line. This study was supported by A\*STAR (Agency for Science, Technology and Research), Singapore, and Grant in aid for promotion of young scientists in cancer research, Japan, while the work of S. C. Kogan on this project was supported by the USA. National Cancer Institute Grant U01-CA84221.

## References

- Akagi, K., Suzuki, T., Stephens, R.M., Jenkins, N.A. & Copeland, N.G. (2004) RCGD: retroviral tagged cancer gene database. *Nucleic Acids Research*, **32**, Database issue D523–527.
- Basecke, J., Cepek, L., Mannhalter, C., Krauter, J., Hildenhausen, S., Brittinger, G., Trumper, L. & Griesinger, F. (2002) Transcription of AML1/ETO in bone marrow and cord blood of individuals without acute myelogenous leukemia. *Blood*, **100**, 2267–2268.
- Bedigian, H.G., Johnson, D.A., Jenkins, N.A., Copeland, N.G. & Evans, R. (1984) Spontaneous and induced leukemias of myeloid origin in recombinant inbred BXH mice. *Journal of Virology*, **51**, 586–594.
- Bedigian, H.G., Shepel, L.A. & Hoppe, P.C. (1993) Transplacental transmission of a leukemogenic murine leukemia virus. *Journal of Virology*, **67**, 6105–6109.

- Castilla, L.H., Wijmenga, C., Wang, Q., Stacy, T., Speck, N.A., Eckhaus, M., Marin-Padilla, M., Collins, F.S., Wynshaw-Boris, A. & Liu, P.P. (1996) Failure of embryonic hematopoiesis and lethal hemorrhages in mouse embryos heterozygous for a knocked-in leukemia gene CBFβ-MYH11. *Cell*, **87**, 687–696.
- DeKoter, R.P., Walsh, J.C. & Singh, H. (1998) PU.1 regulates both cytokine-dependent proliferation and differentiation of granulocyte/macrophage progenitors. *EMBO Journal*, **17**, 4456–4468.
- Erkeland, S.J., Valkhof, M., Heijmans-Antonissen, C., van Hoven-Beijen, A., Delwel, R., Hermans, M.H. & Touw, I.P. (2004) Large-scale identification of disease genes involved in acute myeloid leukemia. *Journal of Virology*, **78**, 1971–1980.
- Gari, M., Goodeve, A., Wilson, G., Winship, P., Langabeer, S., Linch, D., Vandenberghe, E., Peake, I. & Reilly, J. (1999) c-kit proto-oncogene exon 8 in-frame deletion plus insertion mutations in acute myeloid leukaemia. *British Journal of Haematology*, **105**, 894–900.
- Hangaishi, A., Ogawa, S., Imamura, N., Miyawaki, S., Miura, Y., Uike, N., Shimazaki, C., Emi, N., Takeyama, K., Hirokawa, S., Kamada, N., Kobayashi, Y., Takemoto, Y., Kitani, T., Toyama, K., Ohtake, S., Yazaki, Y., Ueda, R. & Hirai, H. (1996) Inactivation of multiple tumor-suppressor genes involved in negative regulation of the cell cycle, MTS1/p16INK4A/CDKN2, MTS2/p15INK4B, p53, and Rb genes in primary lymphoid malignancies. *Blood*, **87**, 4949–4958.
- Hayashi, K., Natsume, W., Watanabe, T., Abe, N., Iwai, N., Okada, H., Ito, Y., Asano, M., Iwakura, Y., Habu, S., Takahama, Y. & Satake, M. (2000) Diminution of the AML1 transcription factor function causes differential effects on the fates of CD4 and CD8 single-positive T cells. *Journal of Immunology*, **165**, 6816–6824.
- Hayashi, K., Yamamoto, M., Nojima, T., Goitsuka, R. & Kitamura, D. (2003) Distinct signaling requirements for Dmu selection, IgH allelic exclusion, pre-B cell transition, and tumor suppression in B cell progenitors. *Immunity*, **18**, 825–836.
- Higuchi, M., O'Brien, D., Kumaravelu, P., Lenny, N., Yeoh, E.J. & Downing, J.R. (2002) Expression of a conditional AML1-ETO oncogene bypasses embryonic lethality and establishes a murine model of human t(8;21) acute myeloid leukemia. *Cancer Cell*, **1**, 63–74.
- Ichikawa, M., Asai, T., Saito, T., Seo, S., Yamazaki, I., Yamagata, T., Mitani, K., Chiba, S., Ogawa, S., Kurokawa, M. & Hirai, H. (2004) AML-1 is required for megakaryocytic maturation and lymphocytic differentiation, but not for maintenance of hematopoietic stem cells in adult hematopoiesis. *Nature Medicine*, **10**, 299–304.
- Imamura, J., Miyoshi, I. & Koeffler, H.P. (1994) p53 in hematologic malignancies. *Blood*, **84**, 2412–2421.
- Jonkers, J. & Berns, A. (1996) Retroviral insertional mutagenesis as a strategy to identify cancer genes. *Biochimica et Biophysica Acta*, **1287**, 29–57.
- Kogan, S.C., Ward, J.M., Anver, M.R., Berman, J.J., Brayton, C., Cardiff, R.D., Carter, J.S., de Coronado, S., Downing, J.R., Fredrickson, T.N., Haines, D.C., Harris, A.W., Harris, N.L., Hiai, H., Jaffe, E.S., MacLennan, I.C., Pandolfi, P.P., Pattengale, P.K., Perkins, A.S., Simpson, R.M., Tuttle, M.S., Wong, J.F. & Morse, III, H.C. (2002) Bethesda proposals for classification of nonlymphoid hematopoietic neoplasms in mice. *Blood*, **100**, 238–245.
- Liu, P., Tarle, S.A., Hajra, A., Claxton, D.F., Marlton, P., Freedman, M., Siciliano, M.J. & Collins, F.S. (1993) Fusion between transcription factor CBFβ/PEBP2β and a myosin heavy chain in acute myeloid leukemia. *Science*, **261**, 1041–1044.
- Look, A.T. (1997) Oncogenic transcription factors in the human acute leukemias. *Science*, **278**, 1059–1064.
- Matsuno, N., Osato, M., Yamashita, N., Yanagida, M., Nanri, T., Fukushima, T., Motoji, T., Kusumoto, S., Towatari, M., Suzuki, R., Naoe, T., Nishii, K., Shigesada, K., Ohno, R., Mitsuya, H., Ito, Y. & Asou, N. (2003) Dual mutations in the AML1 and FLT3 genes are associated with leukemogenesis in acute myeloblastic leukemia of the M0 subtype. *Leukemia*, **17**, 2492–2499.
- Michaud, J., Wu, F., Osato, M., Cottles, G.M., Yanagida, M., Asou, N., Shigesada, K., Ito, Y., Benson, K.F., Raskind, W.H., Rossier, C., Antonarakis, S.E., Israels, S., McNicol, A., Weiss, H., Horwitz, M. & Scott, H.S. (2002) In vitro analyses of known and novel RUNX1/AML1 mutations in dominant familial platelet disorder with predisposition to acute myelogenous leukemia: implications for mechanisms of pathogenesis. *Blood*, **99**, 1364–1372.
- Mori, H., Colman, S.M., Xiao, Z., Ford, A.M., Healy, L.E., Donaldson, C., Hows, J.M., Navarrete, C. & Greaves, M. (2002) Chromosome translocations and covert leukemic clones are generated during normal fetal development. *Proceedings of the National Academy of Sciences of the United States of America*, **99**, 8242–8247.
- Okada, H., Watanabe, T., Niki, M., Takano, H., Chiba, N., Yanai, N., Tani, K., Hibino, H., Asano, S., Mucenski, M.L., Ito, Y., Noda, T. & Satake, M. (1998) AML1(−/−) embryos do not express certain hematopoiesis-related gene transcripts including those of the PU.1 gene. *Oncogene*, **17**, 2287–2293.
- Okuda, T., van Deursen, J., Hiebert, S.W., Grosveld, G. & Downing, J.R. (1996) AML1, the target of multiple chromosomal translocations in human leukemia, is essential for normal fetal liver hematopoiesis. *Cell*, **84**, 321–330.
- Osato, M. (2004) Point mutations in the RUNX1/AML1 gene: another actor in RUNX leukemia. *Oncogene*, **23**, 4284–4296.
- Osato, M., Asou, N., Abdalla, E., Hoshino, K., Yamasaki, H., Okubo, T., Suzushima, H., Takatsuki, K., Kanno, T., Shigesada, K. & Ito, Y. (1999) Biallelic and heterozygous point mutations in the runt domain of the AML1/PEBP2αB gene associated with myeloblastic leukemias. *Blood*, **93**, 1817–1824.
- Preudhomme, C., Warot-Loze, D., Roumier, C., Gardel-Duflos, N., Garand, R., Lai, J.L., Dastugue, N., Macintyre, E., Denis, C., Bauters, F., Kerckaert, J.P., Cosson, A. & Fenaux, P. (2000) High incidence of biallelic point mutations in the Runt domain of the AML1/PEBP2αB gene in Mo acute myeloid leukemia and in myeloid malignancies with acquired trisomy 21. *Blood*, **96**, 2862–2869.
- Rhoades, K.L., Hetherington, C.J., Harakawa, N., Yergeau, D.A., Zhou, L., Liu, L.Q., Little, M.T., Tenen, D.G. & Zhang, D.E. (2000) Analysis of the role of AML1-ETO in leukemogenesis, using an inducible transgenic mouse model. *Blood*, **96**, 2108–2115.
- Scheijen, B. & Griffin, J.D. (2002) Tyrosine kinase oncogenes in normal hematopoiesis and hematological disease. *Oncogene*, **21**, 3314–3333.
- Song, W.J., Sullivan, M.G., Legare, R.D., Hutchings, S., Tan, X., Kufrin, D., Ratajczak, J., Resende, I.C., Haworth, C., Hock, R., Loh, M., Felix, C., Roy, D.C., Busque, L., Kurnit, D., Willman, C., Gewirtz, A.M., Speck, N.A., Bushweller, J.H., Li, F.P., Gardiner, K., Poncz, M., Maris, J.M. & Gilliland, D.G. (1999) Haploinsufficiency of CBFA2 causes familial thrombocytopenia with propensity to develop acute myelogenous leukaemia. *Nature Genetics*, **23**, 166–175.
- Speck, N.A. & Gilliland, D.G. (2002) Core-binding factors in hematopoiesis and leukaemia. *Nature Reviews Cancer*, **2**, 502–513.
- Sun, W. & Downing, J.R. (2004) Haploinsufficiency of AML1 results in a decrease in the number of LTR-HSCs while simultaneously in-

- ducing an increase in more mature progenitors. *Blood*, **104**, 3565–3572.
- Suzuki, T., Shen, H., Akagi, K., Morse, H.C., Malley, J.D., Naiman, D.Q., Jenkins, N.A. & Copeland, N.G. (2002) New genes involved in cancer identified by retroviral tagging. *Nature Genetics*, **32**, 166–174.
- Thiede, C., Steudel, C., Mohr, B., Schaich, M., Schakel, U., Platzbecker, U., Wermke, M., Bornhauser, M., Ritter, M., Neubauer, A., Ehninger, G. & Illmer, T. (2002) Analysis of FLT3-activating mutations in 979 patients with acute myelogenous leukemia: association with FAB subtypes and identification of subgroups with poor prognosis. *Blood*, **99**, 4326–4335.
- Turcotte, K., Gauthier, S., Mitsos, L.M., Shustik, C., Copeland, N.G., Jenkins, N.A., Fournet, J.C., Jolicoeur, P. & Gros, P. (2004) Genetic control of myeloproliferation in BXH-2 mice. *Blood*, **103**, 2343–2350.
- Yanagida, M., Osato, M., Yamashita, N., Huang, L.Q., Jacob, B., Wu, F., Cao, X.M., Nakamura, T., Yokomizo, T., Takahashi, S., Yamamoto, M., Shigesada, K. & Ito, Y. (2005) Increased dosage of Runx1/AML1 acts as a positive modulator of myeloid leukemogenesis in BXH2 mice. *Oncogene*, **24**, 4477–4485.
- Yergeau, D.A., Hetherington, C.J., Wang, Q., Zhang, P., Sharpe, A.H., Binder, M., Marin-Padilla, M., Tenen, D.G., Speck, N.A. & Zhang, D.E. (1997) Embryonic lethality and impairment of haematopoiesis in mice heterozygous for an AML1-ETO fusion gene. *Nature Genetics*, **15**, 303–306.
- Zeisig, B.B., Garcia-Cuellar, M.P., Winkler, T.H. & Slany, R.K. (2003) The oncoprotein MLL-ENL disturbs hematopoietic lineage determination and transforms a biphenotypic lymphoid/myeloid cell. *Oncogene*, **22**, 1629–1637.